# Wake Effects when Estimating Residual Life of Wind Turbine Support Structures

**Other Conference Item**

**Author(s):**
Barahona Garzón, Braulio; Chatzi, Eleni

**Publication date:**
2017

**Permanent link:**
https://doi.org/10.3929/ethz-b-000126765

ETH ZÜRICH
CHAIR OF STRUCTURAL MECHANICS
DEPT. OF CIVIL, ENVIRONMENTAL AND GEOMATIC ENGINEERING

# Wake effects when estimating residual life of wind turbine support structures

B. Barahona[*] and E.N. Chatzi[*]

[*]ETH Zürich
Institute for Structural Engineering
Stefano-Franscini-Platz 5
8093 Zürich



*How to cite (IEEE):*
B. Barahona, and E. N. Chatzi. ”Wake effects when estimating residual life of wind turbine support structures,” presented at IMAC-XXXV Conference and Exposition on Structural Dynamics, Garden Grove, CA, 2017.

# Wake Effects when Estimating Residual Life of Wind Turbine Support Structures

B. Barahona[1] and E.N. Chatzi[1]
[1]Institute of Structural Engineering, Department of Civil, Environmental and Geomatic Engineering,
ETH Zürich, Zürich, Switzerland

## ABSTRACT

For efficient diagnostics of the structural health (SHM) of wind turbine structures, it is essential to ensure a good understanding of operating conditions across the design envelope. Operating conditions however vary significantly depending on the layout, the terrain and the atmospheric conditions on site. In larger wind plants in particular, featuring large diameter rotors, flow distortion (i.e., wake effects) among turbines may yield notable impact on power production and acting loads. Moreover, the highly non-stationary nature of wind loading renders the system identification and damage detection tasks non-trivial. A bi-component SHM framework to account for short- and long-term variability has been introduced. Our intention is to further enhance it to account for the interactions with other turbines. In this study we focus on the long(er)-term loads induced by wake effects when the turbine is operating in power production mode. Applying coarse resolution models we estimate the relative impact that wind conditions bear on the loads of the support structure. The application of the proposed methodology for an operating SHM system, is illustrated via a simulated experiment for an arbitrary wind plant with prescribed site conditions.

**Keywords**: Wind turbine support structure, fatigue assessment, residual life, parametric models, wakes

## INTRODUCTION

For efficient diagnostics of the structural health of wind turbine structures, it is essential to ensure a good understanding of operating conditions across the design envelope. Operating conditions however vary significantly, even within the wind farm, depending on the layout, the terrain and the atmospheric conditions on site. In larger wind plants in particular, featuring large diameter rotors, flow distortion (i.e., wake effects) among turbines may yield notable impact on power production and acting loads [1]. Moreover, the highly non-stationary nature of wind loading renders the system identification and damage detection tasks non-trivial.

A bi-component structural health monitoring (SHM) framework to account for short- and long-term variability has been introduced in [2]. In this study we focus on the long(er)-term loads induced by wake effects when the turbine is operating in power production mode. In this context, the residual life is estimated by weighting the damage induced from a subset of design load cases on the basis of the long-term distribution of the wind. For this purpose we apply coarse resolution models, further described in Section , in order to estimate the relative impact that wind conditions such as wind speed, direction and turbulence intensity, bear on the loads of the support structure. We then derive parametric models of the load distributions, with a procedure similar the one described in [3], which allows for obtaining statistical maps of fatigue damage accumulation in different turbines within a given wind plant in a given site.

In order to illustrate the application of the proposed methodology for an operating SHM system, in Section , a simulated experiment is performed for an arbitrary wind plant with prescribed site conditions. The site is mainly defined by the long-term probability distribution of mean wind speed and direction and a given wind plant layout. Finally, we illustrate the calculation of residual life and the relative impact of wake effects.

## MODELS AND METHODS

### Coarse resolution models

Models of wind turbine and plant dynamic response span in fidelity from those used for design verification and analysis of wind turbines, to those applied in wind farm layout and control optimisation. Depending on the specific task, different subdomains are modelled with different fidelity. Namely, for design verification current design standards prescribe high fidelity aero-elastic simulations over an envelope of design cases, but the influence of wakes is only accounted for by means of a site suitability assessment in which an effective turbulence intensity, higher than the ambient turbulence, is prescribed. For layout and control optimisation, coarse resolution models of the whole farm are applied, which typically include quasi-static aerodynamics and state-space models of wind turbines, 2D wind field, and semi-empirical wake models. Several implementations of such models exist, we adopt the Aeolus toolbox [4], with corresponding models briefly described next.

### Wind Turbine

The wind turbine is modeled via quasi-static aerodynamics and dynamics models of torsion in the drive train, generator torque, blade angle control actuator and tower bending. Such models comprise a set of differential and algebraic equations (Equations 1). Table 1 summarizes the main variables and parameters.

$$\begin{aligned}
M_s &= \frac{1}{2} u_r^3 \rho A_r C_P(\lambda_R, \beta) \Omega^{-1} \\
F_T &= \frac{1}{2} u_r^3 \rho A_r C_T(\lambda_R, \beta) \\
\dot{\Omega} &= \frac{1}{J_r} \left( M_s - \phi_s K_s - \dot{\phi}_s B_s \right) \\
\dot{\omega} &= \frac{1}{J_g} \left( -M_g + \phi_s \frac{K_s}{N} + \dot{\phi}_s \frac{B_s}{N} \right) \\
\dot{\phi}_s &= \Omega - \frac{\omega}{N} \\
\dot{M}_g &= \frac{1}{\tau_g} \left( \frac{P_{\text{ref}}}{\omega} - M_g \right) \\
\ddot{z} &= \frac{1}{m_t} \left( F_T - K_t z - B_t \dot{z} \right)
\end{aligned} \tag{1}$$

### Wind and Wakes

A 2-D wind field at hub height is modeled using a single point spectrum and a coherence function, known as the Sandia or Veers method. The spectrum describes the frequency characteristics of a given component $k$ of the wind field at a given point. The coherence function describes the correlation as a function of spatial separation, mean wind speed, and frequency. Equations 2 describe the Kaimal Spectrum and coherence function, which are applied to generate time series considering that the turbulence structure is Frozen (i.e., Taylor's frozen turbulence).

$$\begin{aligned}
S_k(f) &= \sigma_k^2 \left( \frac{4 \frac{L_k}{u_h}}{\left(1 + 6f \frac{L_k}{u_h}\right)^{5/3}} \right) \\
C_k(f) &= \exp\left( -c_k f \frac{l}{u_h} \right)
\end{aligned} \tag{2}$$

A more realistic simulation method for the wind field at the farm level is the complex cross-spectral method [5], which computes the cross-spectrum amongst wind turbines. The coherence parameter between turbines $r$ and $c$, the delay from turbine to turbine

$\tau_{rc}$, and the cross-spectrum $S_{rc}(f)$ are computed [1] with Equations 3.

$$\begin{aligned} S_{rc}(f) &= C_{rc}(f)\sqrt{S_{rr}(f)S_{cc}(f)}\exp -j2\pi f\tau_{rc} \\ c_{rc} &= \sqrt{(c_{xx}\cos\alpha)^2 + (c_{xy}\sin\alpha)^2} \\ \tau_{rc} &= \frac{d_{rc}\cos\alpha}{u_h} \end{aligned} \tag{3}$$

The wake effects considered are wind speed deficit, expansion of the wake width, meandering of wake center line, and wake merging.[2] The mean wind speed deficit $\tau_w$ downwind of a rotor, the wake expansion radius $e$, and wake merging are estimated based on Fransen's model. $\tau_w$ at a distance $d$ depends on the ambient wind speed $u_x$, the thrust coefficient $C_T$, and the wake width $D$. The wake expansion radius $e$, which defines $D$, is in turn a parametric equation as shown in Equations 4. Table 2 summarizes the main parameters and variables in the wind and wake models.

$$\begin{aligned} \tau_w &= u_x - u(d) \approx \frac{1}{2}u_x C_T \left(\frac{\phi_r}{D(d)}\right)^2 \\ e(d) &= \frac{1}{2}\left(\beta_0^{\frac{k_w}{2}} + \alpha_w \frac{d}{\phi_r}\right)^{\frac{1}{k_w}} \\ \beta_0 &= \frac{1+\sqrt{1-C_T}}{2\sqrt{1-C_T}} \end{aligned} \tag{4}$$

### Parametric Models for Estimating Residual Life

We revisit the parametric models as a means to model the wind turbine response over a wide variety of wind conditions. [3] proposed a method to estimate fatigue loads with parametric models. They focused on blade flap- and edge-wise blade root moments. Based on measurements at high wind speeds (15 to 19 $\mathrm{ms}^{-1}$) they derive parametric models of statistical moments ($\mu_i$) to fit short-term probability distributions $f(x)$, which are then weighted by the long-term distribution of wind speed $f(U)$ to estimate a lifetime load distribution $F(x)$. The workflow is as follows

1. Identify a probability distribution suited to fit load ranges $L_r$ of 10-min time series, discarding low amplitude ranges which have negligible effect on damage, a quadratic Weibull distribution is found suitable.
2. Map the parameters of the distribution to a power law function of wind speed $U$ and turbulence intensity $I$ by linear regression
$$\hat{\mu}_i = a_i \left(\frac{U}{U_{\text{ref}}}\right)^{b_i} \left(\frac{I}{I_{\text{ref}}}\right)^{c_i} \tag{5}$$
where $U_{\text{ref}}$ and $I_{\text{ref}}$ are the geometrical means of the data set.
3. Model short-term load distribution $f(L_r)$ with $\hat{\mu}_1$, $\hat{\mu}_2$, and $\hat{\mu}_3$.
4. Estimate lifetime load distribution $F(L_r)$ by weighting with $f(U)$
$$F(L_r) = \int f(L_r|U, I) f(U) dU \tag{6}$$

In this work we focus on the tower fore-aft bending moment, using the models described in Sections -. We simulate bending moments in several turbines exposed to different wind conditions, then follow the previous workflow but extend the analysis to (*i*) a wider range of wind speeds and (*ii*) add the dimension of wind direction to account for wakes. The wind speed is considered to be Weibull distributed (Equation 7), while the wind direction distribution is described by a wind rose as shown in Figure 2.

$$f(U) = \frac{k}{a}\frac{U}{a}^{(k-1)} \exp(-(\frac{U}{a})^k) \tag{7}$$

We define residual life $L_{\text{res}}$ as the remaining of the design life $L_D$ and the accumulated damage equivalent load $L_{\text{eq}}$.

[1] [6] refers to this wind model as *SWF No Taylor*, and to the Sandia Method as *SWF Taylor*.

[2] Similarly to the two wind models, [6] refers to two implementations of the wake effects, *SWF Taylor* is the coarser one based on Jensen's models and *SWF No Taylor* is based on Frandsen's models.

## CASE STUDY

A wind farm consisting of 4 5MW wind turbines is defined for this study, as illustrated in Figure 1. It is assumed that the wind farm is located at a site with a long-term wind speed and direction distribution as illustrated in Figure 2. The motivation for the selection of this layout is to capture the different wake situations, and to resemble a fairly good wind farm layout for a site with (*i*) a South-West main wind direction aligning with the $x$-direction in the layout sketch; (*ii*) uneven distribution of the wind turbines attributed to topographic constraints; and (*iii*) fairly well spaced turbines, particularly along the mean wind direction. WT2 and WT3 are located at $(x, y) = (0, 4\phi_r)$ and $(x, y) = (0, 6\phi_r)$ from WT1, and WT4 is located at $(x, y) = (6\phi_r, 3\phi_r)$ from WT1.

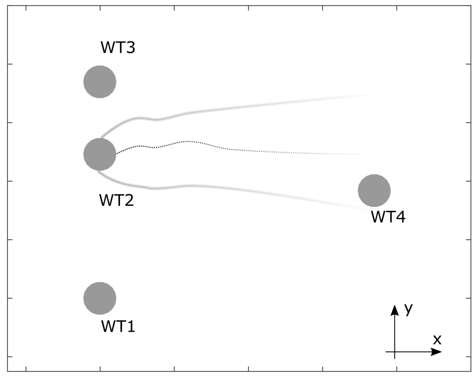


**Fig. 1** Wind farm layout sketch: main wind direction of the site coincides with $x$-axis.

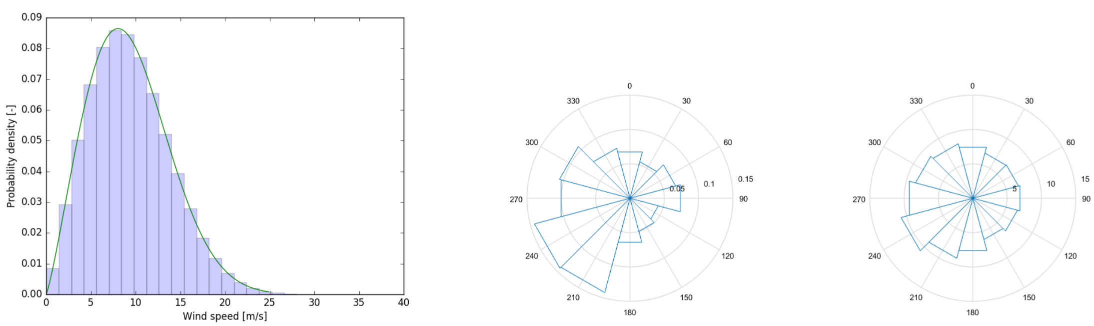


**Fig. 2** Wind speed distribution, wind direction rose, and wind speed rose.

For simplicity in this work we consider wake conditions to be represented by two main cases. Wind blowing from South-West, which is the main wind direction, is the low wake condition as most turbines are free from the distortion of others. Wind blowing from South-East is considered as the large wake condition. These two wind directions are meant to represent the overall wake effects. Sampling from the Weibull distribution $f(U)$ of the wind speed (Equation 7 and left plot in Figure 2) in the range from 6 to 18 ms$^{-1}$ for these two main wind directions, we derive a load envelope over a wide variety of conditions. This is indicated by the probability of exceedance diagrams in Figure 3, where for the two cases simulated rainflow load ranges $L_r$ of all the turbines are plotted in grey. The summary of the farm load envelope for each turbine is shown in black by means of the binned average. We can distinguish a faint tendency of higher loads at larger $L_r$ for wind turbines located down stream of other turbines. Namely, WT4 for South-West wind; and WT2, WT3 for South-East. However, larger larger load ranges $L_r$ correlate to some extend wind mean wind speed, therefore to account for the long-term effects we need to weight with $f(U)$.

Following the workflow described in Section , a first step is to identify a suitable probability function that can be parametrized. Figure 4 shows a log-transform plot of a realisation of $L_r$ and the corresponding fit. Note that compared to the study in [3] (i.e., blade root loads of a single turbine at a high wind speed range) the probability of exceedance is not as well represented by a Weibull fit to the truncated $L_r$. This is further illustrated in Figure 5 and Figure 6 where the statistical moments prove to be a function of wind speed. Notice also that for the case of low wake effects the moments of WT1 and WT2 show, as expected, a

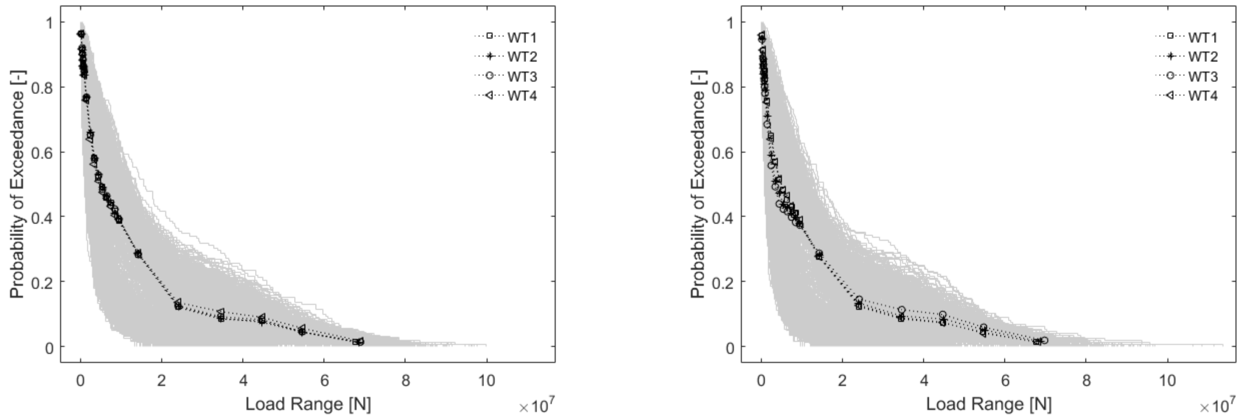


**Fig. 3** Envelope of load ranges $L_r$: left main wind direction from South-West (low wake, 285 10-min time series), right main wind direction from South-East (large wake, 291 10-min time series)

similar trend to wind speed. In the case of larger wake effects a similar trend amongst WTs is revealed, but with different mean and slope at different wind speed ranges. This would result in different parametric models for each turbine and wind speed range.

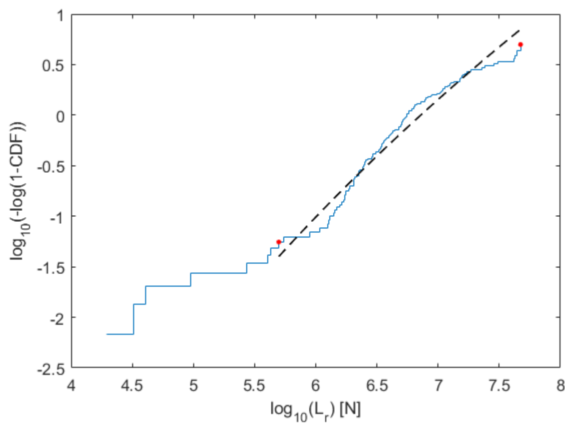


**Fig. 4** Weibull fit

Moving on to the estimation of residual life, Table 3 indicates the residual life estimates based on the simulated loads. For these estimates, the accumulated damage is normalized relative to the free wake condition. The free wake condition is defined with the main wind direction from South-West (aligned with $x$-axis in Figure 1). The tables shows that WT4 is the one exposed to higher loads overall, during different wind speeds and wind directions.

## SUMMARY AND DISCUSSION

Coarse resolution and parametric models of loads can provide trends of the damage accumulation on structures. These physics based models can aid SHM systems in tracking the performance of the structures over longer time frames thereby supporting decisions for when to schedule maintenance. In the conceptual cased we present, the structures perform differently, one of them (WT4) showing significantly less residual life than the rest. This information can aid in deciding which structure to monitor within a wind farm, or how to map the information from a single wind turbine SHM system to monitor the performance of other turbines. The next steps in this approach are to add fidelity by means of (*i*) larger set of load cases to reduce statistical uncertainty, (*ii*) increase fidelity of physics and parametric models, and (*iii*) updating parametric models with data from SHM system.

## REFERENCES


[1] Churchfield, M. J. , Moriarty, P. J. , Hao, Y. , Lackner, M. A. , Barthelmie, R. , Lundquist, J. K. , and Oxley, G. S. . A comparison of the dynamic wake meandering model, large-eddy simulation, and field data at the Egmond aan Zee Offshore

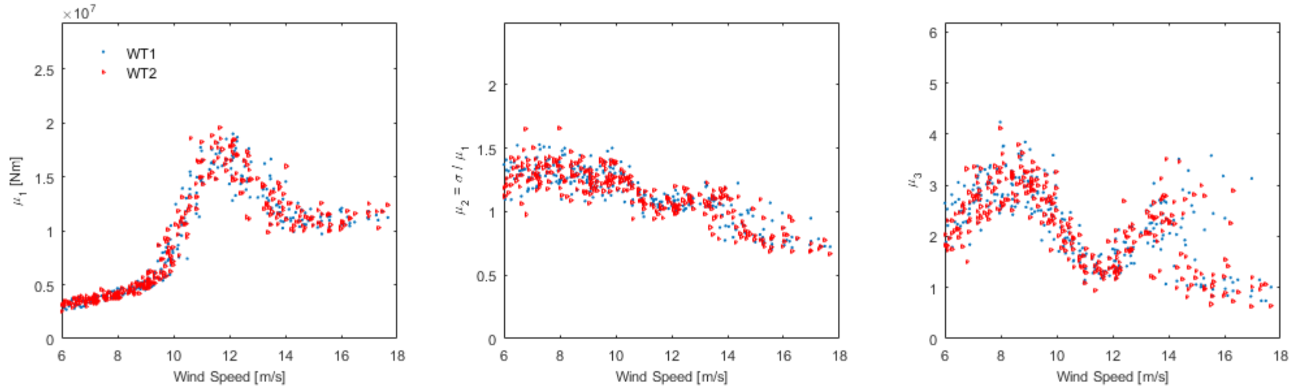


**Fig. 5** Statistical moments of tower fore-aft load ranges simulated in WT1 and WT2 versus mean wind speed (285 samples of the wind from South-West), from left to right: mean $\mu_1$, coefficient of variation $\mu_2$, and skewness $\mu_3$

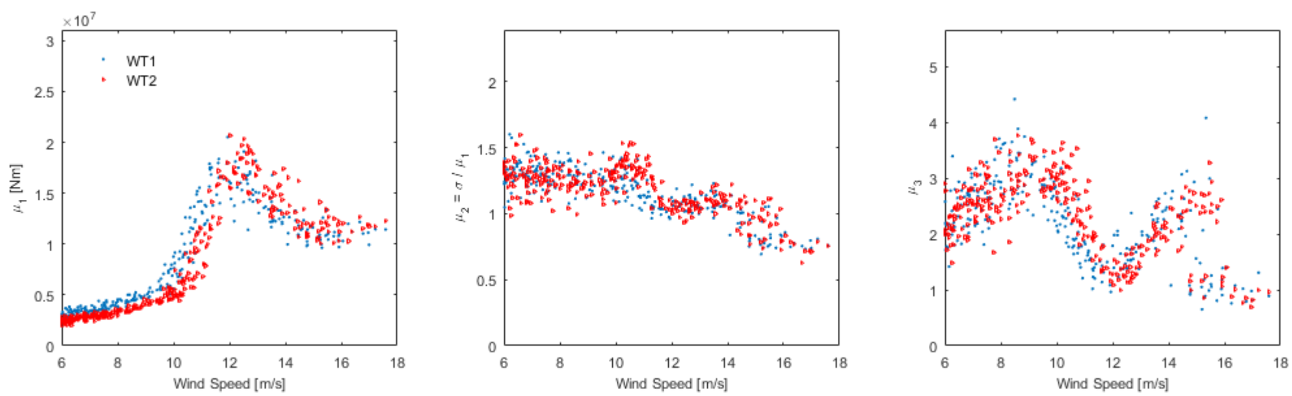


**Fig. 6** Statistical moments of tower fore-aft load ranges simulated in WT1 and WT2 versus mean wind speed (291 samples of the wind from South-East), from left to right: mean $\mu_1$, coefficient of variation $\mu_2$, and skewness $\mu_3$

wind plant. In *AIAA Science and Technology Forum and Exposition (SciTech 2015)*, 2015.

[2] Spiridonakos, M. , Yaowen, O. , Chatzi, E. , and Reiter, U. . Wind turbines structural identification framework for the representation of both short- and long-term variability. In *EMI 2014 Engineering Mechanics Institute Conference (August 5-8)*, 2014.

[3] Manuel, L. , Veers, P. S. , and Winterstein, S. R. . Parametric Models for Estimating Wind Turbine Fatigue Loads for Design. *Journal of Solar Energy Engineering*, 123(4):346–355, 2001.

[4] Grunnet, J. , Soltani, M. , Knudsen, T. , Kragelund, M. , and Bak, T. . *Aeolus Toolbox for Dynamics Wind Farm Model, Simulation and Control*. 2010.

[5] Sørensen, P. , Hansen, A. D. , and Rosas, P. A. C. . Wind models for simulation of power fluctuations from wind farms. *Journal of wind engineering and industrial aerodynamics*, 90(12):1381–1402, 2002.

[6] `http://www.ict-aeolus.eu`. Wind field modeling.

| | | |
|---|---|---|
| $h_h$ | 90 m | Hub height |
| $h_d$ | 3 m | Hub diameter |
| $\phi_r$ | 126 m | Rotor diameter |
| $R$ | $\frac{\phi_r}{2}$ | Rotor radius |
| $A_r$ | $\pi R^2$ | Rotor disc area |
| $\rho_{\text{air}}$ | 1.225 kg m$^{-3}$ | Air density |
| $P_{\text{rated}}$ | 5 MW | Rated power |
| $u_{\text{cut-in}}$ | 3 ms$^{-1}$ | Cut-in wind speed |
| $u_{\text{rated}}$ | 11.4 ms$^{-1}$ | Rated wind speed |
| $u_{\text{cut-out}}$ | 25 ms$^{-1}$ | Cut-out wind speed |
| $\Omega_{\text{cut-in}}$ | 6.9 rpm | Cut-in rotor speed |
| $\Omega_{\text{rated}}$ | 12.1 rpm | Rated rotor speed |
| $u_{\text{nac}}$ | [ms$^{-1}$] | Nacelle wind speed |
| $u_r$ | [ms$^{-1}$] | Average wind speed over the rotor area |
| $u_e$ | [ms$^{-1}$] | Effective wind speed |
| $\omega_m$ | [rpm] | Measured generator rotor speed |
| $\Omega$ | [rad s$^{-1}$] | Rotor speed state |
| $\omega$ | [rad s$^{-1}$] | Generator rotor speed state |
| $\phi_s$ | [rad] | Shaft torsion state |
| $\lambda_R$ | $\frac{R\Omega}{u_\infty}$ | Tip speed ratio |
| $\beta$ | [deg] | Blade pitch angle |
| $\beta_{\text{ref}}$ | [deg] | Blade pitch angle set-point |
| $\beta_m$ | [deg] | Measured blade pitch angle |
| $M_s$ | [Nm] | Main shaft torque state |
| $M_g$ | [Nm] | Generator torque state |
| $F_T$ | [N] | Thrust force |
| $K_s$ | [Nm rad$^{-1}$] | Torsion spring constant |
| $K_t$ | [Nm rad$^{-1}$] | Tower spring constant |
| $B_s$ | [Nm (rad/s)$^{-1}$] | Torsion damping |
| $B_t$ | [Nm (rad/s)$^{-1}$] | Tower damping |
| $N$ | [-] | Gear ratio |
| $J_r$ | [kgms$^{-1}$] | Rotor inertia |
| $J_g$ | [kgms$^{-1}$] | Generator rotor inertia |
| $\tau_g$ | [s] | Generator time constant |
| $P_{\text{dem}}$ | [MW] | Power Demand |
| $P_{\text{ref}}$ | [MW] | Generator power set-point |
| $C_P$ | [-] | Power coefficient: pre-calculated, look-up table given $\lambda_R$ and $\beta$ |
| $C_T$ | [-] | Thrust coefficient: pre-calculated, look-up table given $\lambda_R$ and $\beta$ |

Table 1: Parameters and variables of NREL 5 MW wind turbine model in Aeolus toolbox

| | | |
|---|---|---|
| $L_k$ | [m] | Integral scale parameter: $L_x = 340.2$, $L_y = 113.4$ |
| $f$ | [Hz] | Frequency |
| $u_h$ | [ms$^{-1}$] | Mean wind speed at hub height |
| $\sigma_k$ | [(ms$^{-1}$)$^2$] | Variance: $\sigma_x = Ti(\frac{3u_h}{4} + 5.6)$, $\sigma_y = 0.8\sigma_x$ |
| $l$ | [m] | y-distance in wind field grid |
| $c_k$ | [-] | Coherence parameter: $c_x = 7.1$, $c_y = 4.2$ |
| $\alpha$ | [rad] | Angle between main wind direction and a line between $r$-$c$ |
| $c_{xx}$ | [-] | Auto-coherence parameter in $x$-direction (i.e., $c_x$) |
| $c_{xy}$ | [-] | Cross-coherence parameter between $x$- and $y$-direction |
| $c_{rc}$ | [-] | Cross-coherence parameter between $r$-$c$ |
| $d_{rc}$ | [m] | Distance between $r$-$c$ |
| $\tau_w$ | [ms$^{-1}$] | Mean wind speed deficit in wake |
| $u_x$ | [ms$^{-1}$] | Mean ambient wind speed |
| $D$ | [m] | Wake width downwind from a turbine |
| $\beta_0$ | [-] | Constant in wake expansion model |
| $\alpha_w$ | [-] | Parameter in wake expansion model: $\alpha_w = 0.5$ |
| $k_w$ | [-] | Constant in wake expansion model: $k_w = 2$ |

Table 2: Wind field and wake simulation parameters

| | WT1 | WT2 | WT3 | WT4 |
|---|---|---|---|---|
| $L_{\text{res}}[\%]$ | 1.4 | 3.6 | 3.7 | 0.5 |

Table 3: Estimated residual life in percentage of design life